1-1-2016

Structure Property Relationship of Porcine Adipose Tissue

Ashma Sharma

Structure property relationship of porcine adipose tissue

By

Ashma Sharma

A Thesis
Submitted to the Faculty of
Mississippi State University
in Partial Fulfillment of the Requirements
for the Degree of Master of Science
in Biomedical Engineering
in the Agricultural and Biological Engineering

Mississippi State, Mississippi

August 2016

Structure property relationship of porcine adipose tissue

By

Ashma Sharma

Approved:

_____

Lakiesha N. Williams
(Major Professor)

_____

Rajkumar Prabhu
(Committee Member)

_____

Jun Liao
(Committee Member)

_____

Wes A. Baumgartner
(Committee Member)

_____

Steven H. Elder
(Graduate Coordinator)

_____

Jason Keith
Dean
Bagley College of Engineering

Name: Ashma Sharma

Date of Degree: August 12, 2016

Institution: Mississippi State University

Major Field: Biomedical Engineering

Major Professor: Dr. Lakiesha N. Williams

Title of Study: Structure property relationship of porcine adipose tissue

Pages in Study 48

Candidate for Degree of Master of Science

Adipose tissue, also known as fat tissue are the lipid filled cells with various functions such as, shock absorber, energy storage, and thermal insulation. In this study, the impact of compressive stress at the microstructural level on the porcine abdominal adipose tissue is analyzed under different strain rates of 0.1%, 1%, and 10%. The compressed tissues were fixed in formalin followed by hematoxylin and eosin staining, which were further analyzed at the cellular level using an optical microscope. The preliminary results showed a linear relationship between stress and strain up to 20% strain amplitude. Additionally, the stiffness of the fat tissue was observed to increase with the increase in loading rate. The non-linearity behavior of the adipose tissue and its effects on the cellular level will be studied to understand the mechanical response of fat tissue and its ability to mitigate and absorb energy from low to high strain rate.

DEDICATION

I would like to thank my friends and family members. Without their emotional support and encouragement I wouldn't be here. Also would like to thank my teachers and professors without the knowledge that I got I wouldn't be here.

ACKNOWLEDGEMENTS

I would like to thank all my committee members for the time and thoughts they provided for this work. I am also very thankful to Dr. Lakiesha Williams for providing all the guidance and resources to complete the work. I would also like to thank Dr. Jim Cooley for helping me analyzing and preparing the slides. Also I am very thankful to the pathology department of College of Veterinary Medicine. I am very thankful to MeLanae Garett for training me on Electro force test bench machine. I am also very thankful to Workshop of Agricultural and Biological Engineering Department. This research would not be possible without their help and support.

TABLE OF CONTENTS

LIST OF TABLES

LIST OF FIGURES

CHAPTER I

INTRODUCTION

Athletic and automobile collisions are both common causes of injury. Factors associated with injuries include crash severity, Impact direction, and deformation/damage. Clinical studies show a variability in the injury susceptibility depending on age, coexisting disease, and physical properties of the body tissues.(Wang, Bednarski et al. 2003)

Human bodies are composed of fat, muscle, and other soft and hard biological tissues. The mechanical properties of tissues and organs vary widely. The properties of the heel fat pad have been well studied and was shown to be an effective shock absorber. (Ker, Bennett et al. 1989, Miller-Young, Duncan et al. 2002) The property of fat tissue is also to mitigate the energy which is very important to protect the inner organs. Football players, especially offensive line back, whose average body weight are around 300lb protect the quarterbacks are chubbier which might help them to protect their internal organs. Looking at the structure property relationship of fat help us to design a bioinspired materials.

1.1 Background

Fat Tissue, also known as Adipose Tissue, mainly comprises of loose connective tissue which is located below the dermis layer. The main function of adipose tissue is thermal Insulation, energy storage, shock absorption, and muscle movement.(Comley and

Fleck 2012) The structure and mechanical properties of adipose tissue is Isotropic in nature. Subcutaneous tissue is a tissue that can be found in between the dermis, aponeurosis, and fascia of the muscle. (Comley and Fleck 2010) Adipose tissue is almost like a connective tissue where fat cells are deposited inside the extra cellular matrix. (Wertheimer and Shapiro 1948) Adipose tissue also known as an active metabolic endocrine organ, is a metabolic sites for different hormone and proteins such as steroid hormone and glucocorticoid hormone. (Kershaw and Flier 2004)

Fat tissue have different mechanical properties regarding its association with and without skin. Their stiffness is slightly different from one another with regard to skin but the pattern of curve in stress strain diagram that skin follows and fat tissue follows is the same. (Wu, Cutlip et al. 2007) Also the thickness of the skin might somehow effect the mechanical behavior of adipose tissue. (Iivarinen, Korhonen et al. 2014)

Fat tissue is composed of adipocytes, vascular endothelial cell which can be found where there is loose connective tissue. There are two kind of adipose tissues-- brown adipose tissue and white adipose tissue. They differ slightly in their morphology and properties. The difference between brown adipose and white adipose tissue is brown adipose tissue are rich in mitochondria and poor in lipids while white adipose tissue are rich in lipids and poor in mitochondria. White adipose tissue stores energy while brown adipose tissue expends energy. (Cahill and Renold 1965) The fat is distributed in a wide range throughout the body. Subcutaneous and visceral are the two different kinds of fat based on the distribution in the body. Their percentage vary throughout the body. (Abraham, Pedley et al. 2015)

1.2 Morphology and Extra Cellular Matrix

Adipose Tissue is made up of lipid filled cells known as adipocytes. Adipose tissue of healthy adults contain one third of the mature adipocytes. Each Adipose Cell consists of one lipid vacuole, a nucleus and a phospholipid bilayer. Each Adipocyte is supported by two collagen based structures. Mainly type I and type IV collagen is found in adipose tissue. (Comley and Fleck 2010) Adipose tissue just beneath the skin, which is also known as subcutaneous region, is a soft connective tissue made up of a collagen fiber network. (Comley and Fleck 2010)

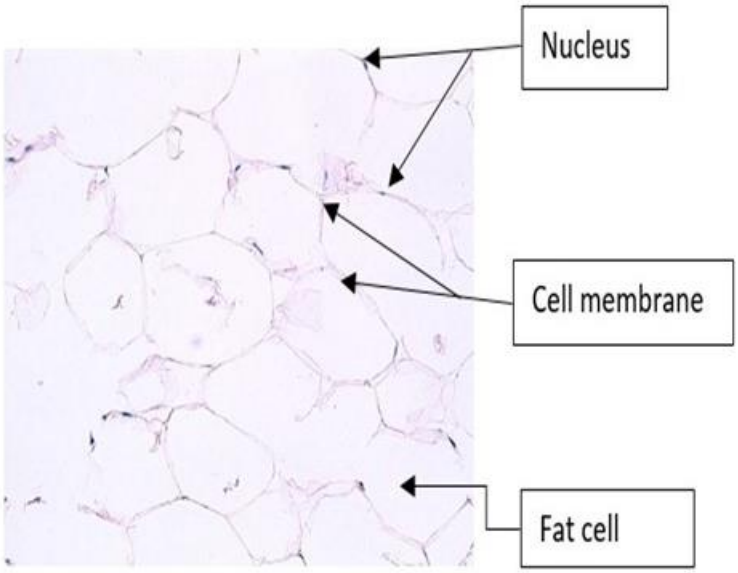

Figure 1.1 Fat tissue with label in Hematoxylin and Eosin Staining

Adipose Tissue is supported by two layers externally. The reinforcement basement membrane is mainly a type IV collagen mesh, which behaves as closed cell foam.(Comley and Fleck 2010) The other layer is the interlobular septa, made of type 1 collagen, and acts as an open cell 3D foam, and has a negligible contribution mechanical

response and stiffness at the macroscopic level as shown in Figure 1. (Comley and Fleck 2010, Sommer, Eder et al. 2013)

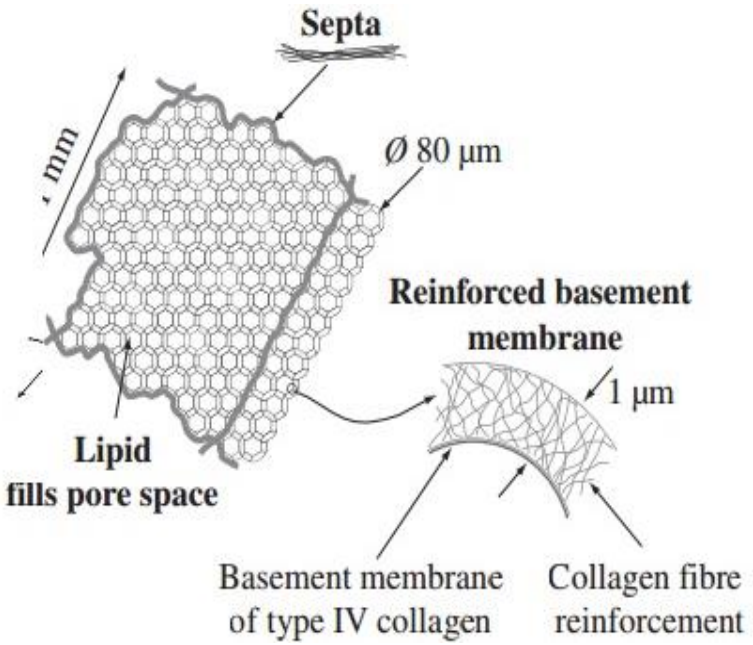

Figure 1.2 A sketch of a lobule of adipose tissue (Comley and Fleck 2010)

The fat or lipid inside the extracellular matrix of fat tissue is viscous material which stores the energy known as Triacylglycerol. They are normally arranged in random order and entirely surrounded by basement membrane as shown in Figure 1.2.

1.3 Previous Study on Properties of fat tissue

Adipose Tissue can be treated as a non-porous viscoelastic solid. (Tan, Ng et al. 2005) Several studies concluded that the subcutaneous Adipose tissue has some capability of expansion as well as the ability to recover from a mechanical deformation.

(Alkhouli, Mansfield et al. 2013) This study supports the fact that the adipose tissue absorbs energy and helps in protection of muscle.

The relationship between the mechanics and structures might help to determine if elastic or plastic deformation occurs at different strain rates. Adipose tissue has a greater ability to transfer a load between the structures during physical activities including breathing.(Comley and Fleck 2012) According to a study by Geerligs et al., subcutaneous adipose tissue experiences a larger strain than the dermis and it contributes to the mechanical properties of skin . It can also experience a larger strain in vivo. (Geerligs, Peters et al. 2008, Alkhouli, Mansfield et al. 2013)

Adipose tissue plays a very important role in load transfer between the structure in the body during breathing, body movement, and exercise or whenever it is exposed to any therapeutic stretching during physiotherapy and massages. (Geerligs, Peters et al. 2008)

According to the previous studies, the type of tissues that are used in testing can affect the properties of cell.(Tan, Ng et al. 2005) Subcutaneous adipose tissue has somehow similar properties to that of heel pad which are efficient shock absorption and protection.

The main study is to measure the impact on the abdomen part of porcine subcutaneous adipose tissue from control to some vertical load. (Gefen and Haberman 2007) Our main goal is to evaluate the structure property relationships of adipose tissue in compression because of its role as a shock absorber. (Alkhouli, Mansfield et al. 2013)

Fat is a viscoelastic materials and behaves as non-linear viscoelastic solid while under compressive loading. Mechanical testing has been performed on porcine adipose

tissue at many levels of strain rates. The energy dissipation density is lower in subcutaneous Adipose tissue compared to other dermis layers. (Alkhouli, Mansfield et al. 2013) Therefore, subcutaneous adipose tissue can handle more deformation and recover easily from mechanical damage. Subcutaneous adipose tissue allows for loads to transfer more readily and thus protects the inner organ from damage due to impact. (Patel, Smith et al. 2005)

Many mathematical models were used for the heel pad. The mechanical properties from force deformation might help to find the effect of loading in musco-skeletal system. (Naemi, Chatzistergos et al. 2015) The simplest model reversible elastic deformation tells about the linear elastic model where materials has linear stress strain curve which follows the hooke's law.(Delingette 1998) But some material follow linear elastic model only for the short displacement, if they have higher displacement then stress strain curve is no longer linear. Some tissues during loading unloading, the strain does not reach to zero. That kind of deformation is known as plastic deformation. While most tissue reaches to zero during loading and unloading.(Delingette 1998, Šifta and Bittner 2010)In most of the soft tissue stress is also related to the speed of deformation which is also known as strain rate. These tissue material is considered as viscous. Most soft tissue are viscoelastic, combining both viscosity and elasticity behavior.

Additional studies will provide insight on how adipose tissue will dissipate energy. This will be done through also characterizing the changes in microstructure at the cellular level, which plays a key role in energy absorption and dissipation. Previous studies on heel pad suggests that it is made up of the fat tissue but have slightly different properties. The large dissipation of energy in heel pad material predict around 90%

energy loss in vivo while the pad isolated can only dissipate around 30% energy loss. (Aerts, Ker et al. 1995) The properties of fat also might differ in vivo and in isolated form.

According to Alkhouli et al, Adipose tissue shows a linear mechanical response up to 30% strain. However, the stress strain relation is nonlinear. (Comley and Fleck 2012) At low strain rates the response to compression test is linear up to 30% and after that the stress level increases rapidly. (Comley and Fleck 2010)

Subcutaneous fat usually experiences larger strain than the dermis and its stiffness is smaller than that of dermis. This is likely why it absorbs the energy and protect the inner organs from external damage. (Geerligs, Peters et al. 2008, Alkhouli, Mansfield et al. 2013) The uniaxial test does not address any time dependent property of tissue but when fat and skin are detached then the result might give the property of fat itself which might be more accurate. (Miller-Young, Duncan et al. 2002)

According to the Geerligs and his team, abdominal subcutaneous fat tissue of rats only shows linear viscoelastic behavior only up to 50% when it is under tension. (Geerligs, Peters et al. 2008) The approach while doing the experiment or the methods that would likely be using is the compression test at different strain rates i.e. lowest to highest. The stiffness between all different types of strain rates are compared in order to find out the impact on the tissue due to different strain rates. The porcine subcutaneous adipose tissue is used. The properties and structure of tissue is almost similar to the human adipose tissue.

The area fraction of fat tissue is used to find out the failure due to load, stress and modulus and the strength of the tissue is directly related with the count of cell, size and distribution. (Williams, Elder et al. 2008)

Fat tissue is normally fixed by immersing it to several hours in formalin solution depending on its size. 2-3 mm thick tissue can be fixed in 12 hours. But the texture of the tissue also changes the time for fixation. Then paraffin embedded section from fixed fat cell were stained in hematoxylin and Eosin (H&E) stain by extracting lipid cells. (Tracy and Walia 2002)

1.4 Specific Aim

The objective of this study is to quantify the structure property relationship of Fat tissue at variant strain rate as well as to investigate the design of engineering system.

1. Apply compression testing at various strain rates (0.1/s,0.01/s,0.001/s) to the subcutaneous portion of adipose tissue from the abdominal of adult pigs.
2. Interruption compression testing was applied at all three strain rates at 15% and 30% strain to characterize microstructural changes at these strain levels.
3. Microstructural Characterization: Hematoxylin and Eosin staining was applied to the fat tissue all strain rates to see the changes in the structure of fat based on strain rate and strain level.
4. Area fraction and cell density were quantified for each strain rates level and control and finding the difference.
5. Hysteresis: Energy Dissipation were quantified for each strain rate by repeating loading and unloading compression test.

CHAPTER II

MATERIALS AND METHODS

2.1 Sample Preparation

Porcine fat tissue from healthy adults (6 to 8 month old) with 240 lbs. to 270 lbs. weight were obtained from a local abattoir (Sansing Meat Service, Maben, MS). They were transported to an Agricultural and Biological Engineering department by keeping it in a cooler and wrapped with a gauze along with a Phosphate Buffered saline (Sigma-Aldrich,St. Louis,MO). Phosphate Buffered Saline (PBS) is used to minimize dehydration as well as degradation of tissue. Testing was initiated upon arrival to the Department of Agricultural and Biological Engineering at Mississippi State University. The compression test at different strain rates was completed in the same day using Electroforce Test Bench (BOSE) machine while for interruption testing was completed within three days from the slaughter time. The tissue were wrapped with the gauze and placed in phosphate buffer saline (PBS) in the Refrigerator for three days .The test sample were acquisitioned with the help of scalpel and hollow cylindrical rod. The samples were punched and removed with the custom in-house hollow cylindrical rod whose outer diameter is 25 mm and height approximately 50 mm. The cylindrical samples were then trimmed to 9-13 mm thickness and 24 mm diameter with a scalpel and cylindrical rod respectively, and also the surface were made smooth with the help of the scalpel. The samples were cut in the longitudinal manner in preparation for testing.

Figure 2.1 Fat Tissue with dimension in inches

2.2 Compression Test(Longitudinal)

Compression testing was conducted in the longitudinal orientation (n=21) with the Electroforce Test Bench mechanical testing device (Model 400NLM1TB,New Castle, DE) at three different strain rates 0.001/s, 0.01/s and 0.1/s keeping the strain constant and varying the force. The thickness and the diameter of the sample were measured using a Vernier caliper(accuracy of 0.01 mm). Specimens were then kept moist in the PBS solution before testing and for the duration of testing to avoid dehydration during the experiment. Testing was initiated from zero load and zero strain. The sample was compressed up to 50% in all three strain rates as shown in Figure 2.2. Engineering stress and strain was calculated from force and displacement data obtained from each test. .True Stress and Strain were obtained using equation (2.1) and equation (2.2) respectively.

$$\sigma_T = \sigma_E(1 + \varepsilon_E) \quad (2.1)$$

$$\varepsilon_T = ln(1 + \varepsilon_E) \quad (2.2)$$

where,

ε_E= Engineering Strain and σ_E = Engineering Stress

ε_T = True Strain and σ_T= True Stress

The sample geometry was approximated as a circle. The cross sectional area for each sample was then calculated before the test. Longitudinal compression was done to two different strains (30% and 50%) for each strain rates (n=7) and for repeated loading unloading test was done (n=3) at each strain rates.

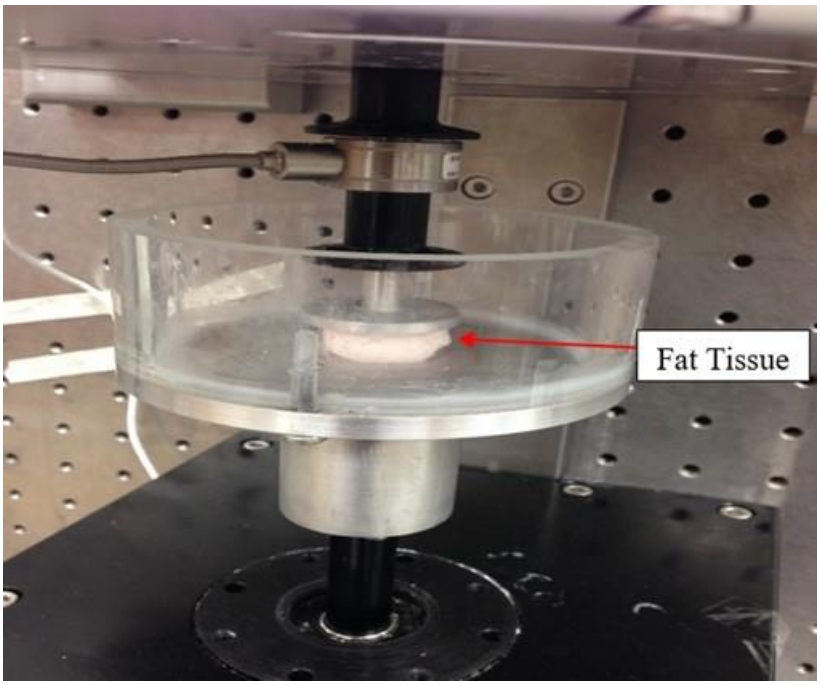

Figure 2.2 Compressing Fat tissue at different strain load in Electroforce Test Bench

2.3 Hysteresis

Compression tests were conducted in the longitudinal direction (n=9) specimen with the Electroforce Test Bench Machine at the three different strain rates 0.1/s, 0.01/s,0.001/s. Loading and unloading were repeated up to 10 cycle. The hysteresis was obtained for repeated loading unloading case. The area of the hysteresis loop was calculated using matlab software. The area under continuous curve can be calculated using equation (2.3)

$$\text{Area} \approx \sum_{i=1}^{N} f_i \Delta x \tag{2.3}$$

where, Δx is length of x for each small rectangle.

f(x) is an equation of a curve as a function of x.

In the same way true stress and strain are calculated and the hysteresis diagram of repeated loading and unloading was obtained by averaging the number of test

2.4 Interruption test

The microstructural changes during loading was also studied in order to evaluate the effect of strain rate and strain level on tissue structure. Samples were prepared in the same way as it was done for the compression test. Nine test conditions were examined for each strain rate and they are 0.001/s, 0.01/s, and 0.1/s. Three control samples, three at 15% engineering strain and three at 30% engineering strain. A total of 27 samples were prepared for the interruption study. The sample was fixed at the target strain level by submerging the sample in Neutral Buffered Formalin immediately when the desired strain level was reached. The sample remained in the fixative at room temperature for approximately 48 hours. The fixed sample was removed and cut in the longitudinal direction and then two halves were cut again in the transverse direction. This was done to

examine different orientation. Figure 2.3 is a schematic to the longitudinal and transverse orientation. The samples were then stained with hematoxylin and eosin (H&E). The stained samples were viewed under Leica DM 2500 microscope (Leica Microsystem, Buffalo Grove, IL).

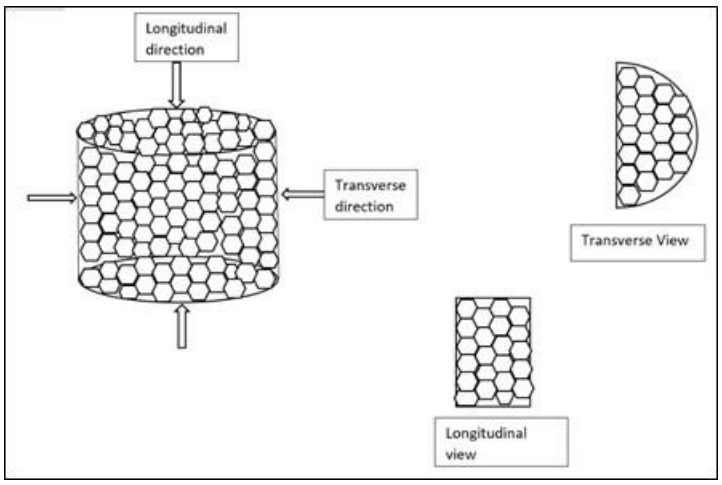

Figure 2.3 Schematic diagram of fat tissue

2.5 Image Analysis

The image obtained from Leica DM 2500 microscope were further analyzed using image J software (National Institutes of Health).Using image J software the number of cells present in the tissue and the area of cells present in the tissue were calculated. With the help of the calculated area and number density, the area fraction for each cells were calculated.

$$Area\ Fraction(AF) = \frac{\text{Total area of cell}(\mu m^2)}{Total\ image\ area(\mu m^2)} \quad (2.4)$$

$$Number\ Density(ND) = \frac{Total\ Number\ of\ cell}{Total\ image\ area(m^2)} \quad (2.5)$$

CHAPTER III

RESULTS

3.1 Compression Testing

Mechanical responses of adipose tissue at varying strain rates and levels were studied. This was done for longitudinal orientations. The data was collectively averaged for each strain rate using a stress-strain graphical user interface (MSU, center for Advanced Vehicular Systems).The stress-strain response for the fat tissue under compression showed the typical nonlinear response for viscoelastic materials (Figure. 5-figure 8). The response was highly linear up to 20% strain. The stress strain response diverge after the initial toe region at around 20% strain.Strain rate dependency which is also the characteristic of soft tissue was observed. The stiffness increased as the strain rate increases. All trend of the curve was the same, independent of strain rate.

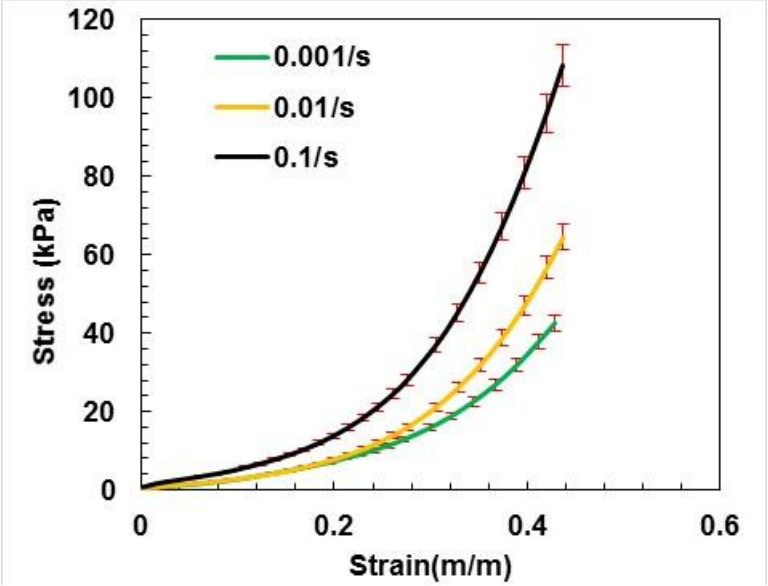

Figure 3.1 Stress-Strain response for fresh fat tissue in compression at longitudinal direction at three different strain rates

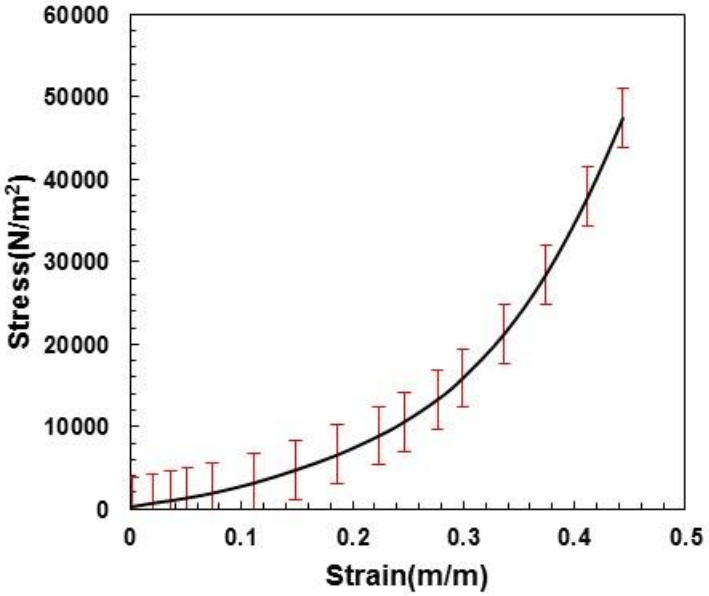

Figure 3.2 Stress Strain Curve with error bar at 0.1/s Strain rate in longitudinal direction

The fat tissue was compressed up to 50% Engineering strain (45% True Strain). The maximum stress of 50000 N/m^2 was obtained at 45% strain as shown in Figure 3.2.Similarly, slope at 0.1/s was 57154.

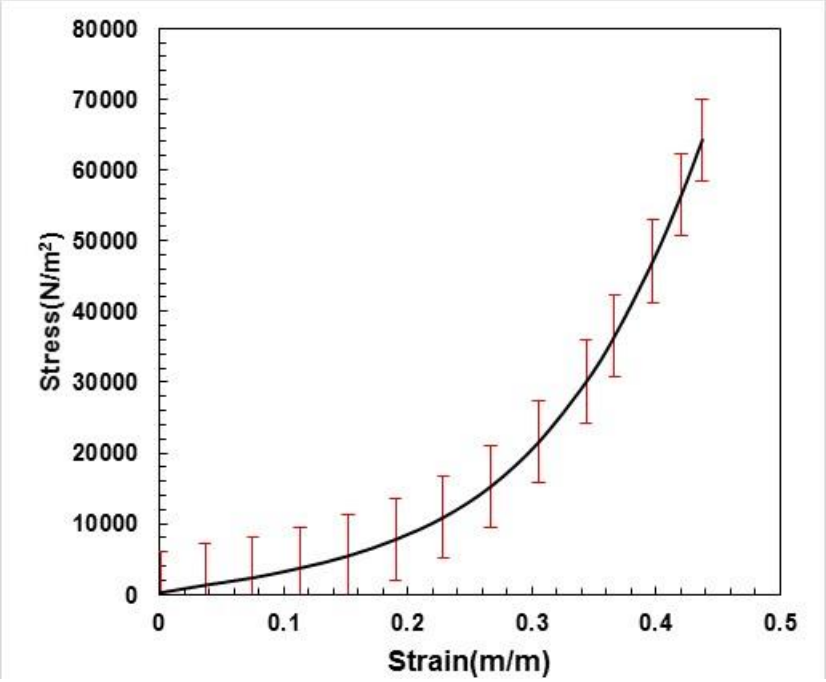

Figure 3.3 Stress Strain Curve with error bar at 0.01/s Strain rate

The same concave like trend across the strain rates. The maximum stress of 65000N/m^2 was obtained at 45% strain at 0.01/s strain rates as shown in Figure 3.3.The slope was 38508 .

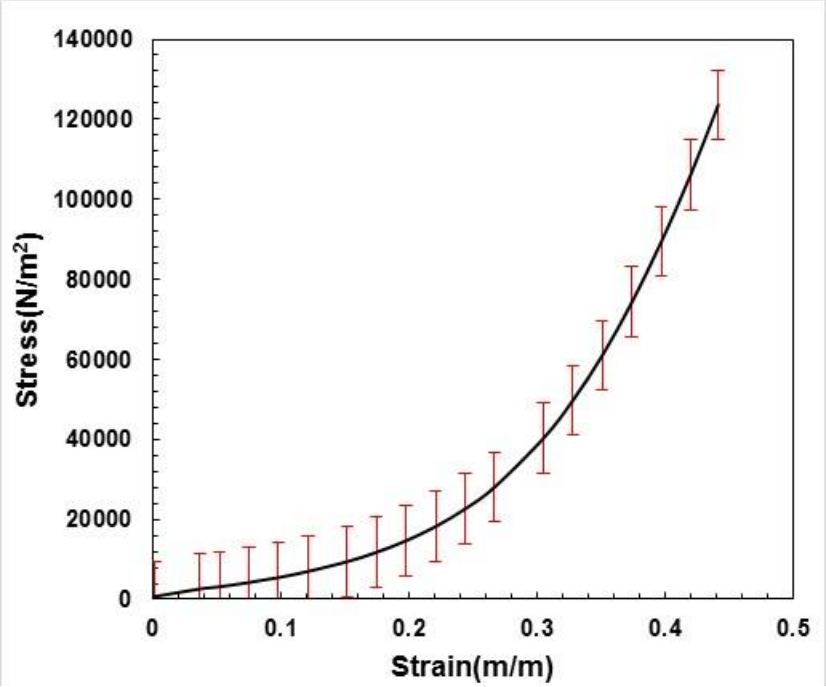

Figure 3.4 Stress Strain Curve with error bar at 0.001/s Strain rate

Stress Strain curve of fat tissue at 0.1/s strain rates along with the standard deviation can be observed in Figure 3.4. When the strain is at 0.2 or 20%, curve is linear. At 0.1/s strain rate, maximum Stress at 40% strain was 130000 N/m^2 and the slope was 29268. According to this result, as the strain rates increases, more amount of stress is obtained to get the same strain.

3.2 Microstructural Characterization and Image Analysis

Image J analysis was conducted with Image J software (National Institutes of Health, Baltimore, MD) open source software. The tissue was stained with H&E and the slides were analyzed using Leica microscope in order to see the changes in the microstructural level of fat tissue. It was performed on sample at all three strain rates, two levels of strain, and two directions for total of n=9 and a control with n=3. The tissue was

then cut in the transverse and longitudinal direction and imaged using Leica microscope. Number density, cell count, mean area and Area fraction was calculated using Image J for all transverse and longitudinal tissue (n=3) and also for all three strain rate.

Table 3.1 Number density, Mean area ,Area fraction and Cell Count

Name	Cell Count	Area fraction	Number Density	Mean Area(mm^2)
Longitudinal 0.1/s(15%)	13.333	0.57556	0.00000676	113933.8
Longitudinal 0.01/s(15%)	13.667	0.564754	0.00000692	111576.4
Longitudinal 0.001/s(15%)	15.333	0.55638	0.00000769	110793.9
Transverse 0.1/s(15%)	11.333	0.603153	0.00000571	119782.2
Transverse 0.01/s(15%)	14.333	0.613899	0.00000728	126105.7
Transverse 0.001/s(15%)	19.333	0.555144	0.00000975	109971.3
Longitudinal 0.1/s (30%)	5.333	0.533783	0.00000269	105566.7
Longitudinal 0.01/s (30%)	8.333	0.542618	0.00000418	108151.7
Longitudinal 0.001/s (30%)	11	0.586678	0.00000554	116470.1
Transverse 0.1/s(30%)	4.333	0.446911	0.00000219	88221.28
Transverse 0.01/s(30%)	5.667	0.497741	0.00000285	99015.91
Transverse 0.001/s(30%)	8.667	0.54268	0.00000436	107863.4
Control Longitudinal	21.25	0.703312	0.000108635	137469.2
Control Transverse	22.75	0.615133	0.000115636	118386.3

Number density, area fraction and mean area are reported in table 1 for six test plus control. The mean area for 15% and 30% strain for all three strain rates are reported

in Table 3.1. A trend is observed in 30% strain that the mean area in longitudinal direction is greater than the mean area in transverse direction in all strain rates, that is at 30% mean area in longitudinal direction for 0.1/s,0.01/s and 0.001/s is 105566.7±32400.18μm^2, 1081551.7±2921.063 μm^2 and 116470.1±4397.95 μm^2 respectively. Similarly, The mean area in transverse direction of longitudinally compressed tissue at 0.1/s,0.01/s and 0.001/s Strain rates are 88221.28±20948.44μm^2, 99015.91±11476.2 μm^2 and 107863.4±14836.05 μm^2 respectively.

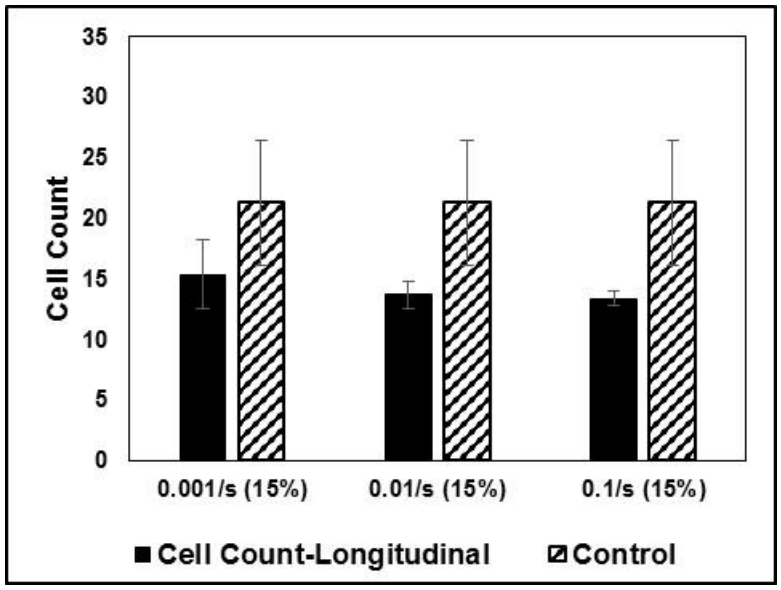

Figure 3.5 Cell Count of control and longitudinal view at 15% strain

The cell count of longitudinal view of compression test at 15% strain of all three strain rates that is 0.1/s,0.01/s and 0.001/s is 13.33±0.577, 13.66±1.1547 and 15.33±2.886751 respectively. The area of control is same for all longitudinal view and it is 21.25±5.123.the less number of cell were observed in 0.1/s compared to control and

0.01/s and 0.001/s strain rates. The Figure 3.5 shows the cell count for all strain rates compared with the control.

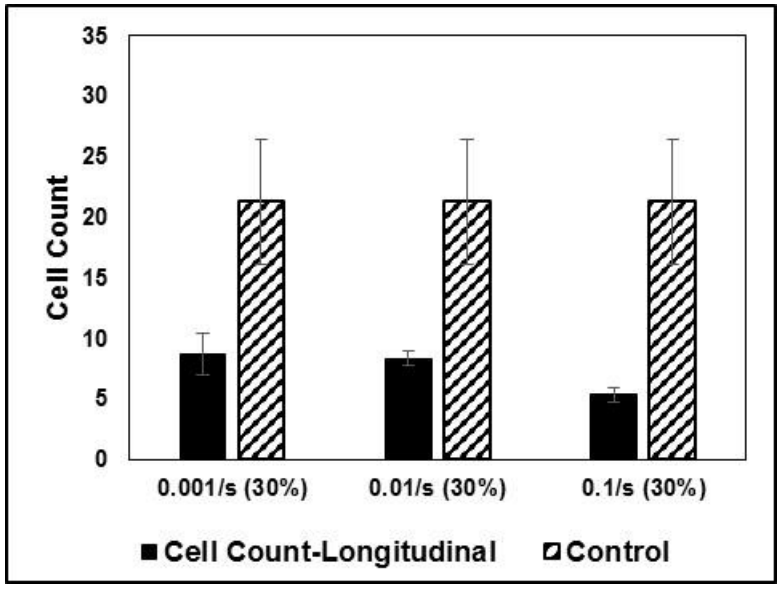

Figure 3.6 Cell Count of control and longitudinal view at 30% strain

The Figure 3.6 shows the cell count for all strain rates compared with the control. The cell count of longitudinal view of compression test at 30% strain of all three strain rates that is 0.1/s,0.01/s and 0.001/s is 13.33±0.577, 13.66±1.1547 and 15.33±2.886751 respectively. At 30% strain, the number of cell compared to control are less.

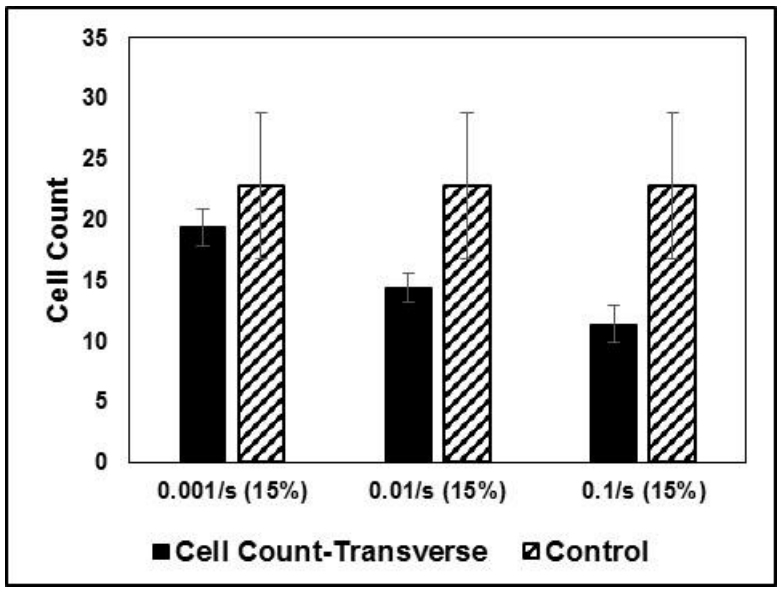

Figure 3.7 Cell Count of control and Transverse view at 15% strain

The Figure 3.7 shows the cell count for all strain rates in the transverse direction compared with the control. The cell count of Transverse view of compression test at 15% strain of all three strain rates that is 0.1/s,0.01/s and 0.001/s is 5.33±0.577, 8.33±1.1547 and 15.33±2.886751 respectively. The area of control is same for all Transverse view and it is 22.75±6.0759. The results obtained were almost similar to that of longitudinal direction.

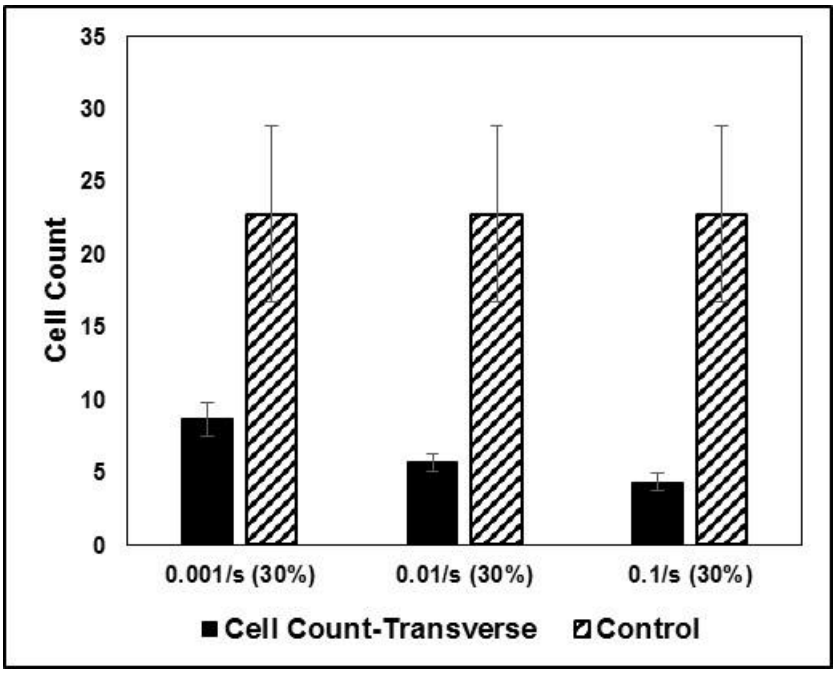

Figure 3.8 Cell Count of control and Transverse view at 30% strain

The Figure 3.8 shows the cell count for all strain rates compared with the control. The cell count of Transverse view of compression test at 30% strain of all three strain rates that is 0.1/s,0.01/s and 0.001/s is 4.33±0.577, 5.667±0.57735 and 8.667±1.154701 respectively.

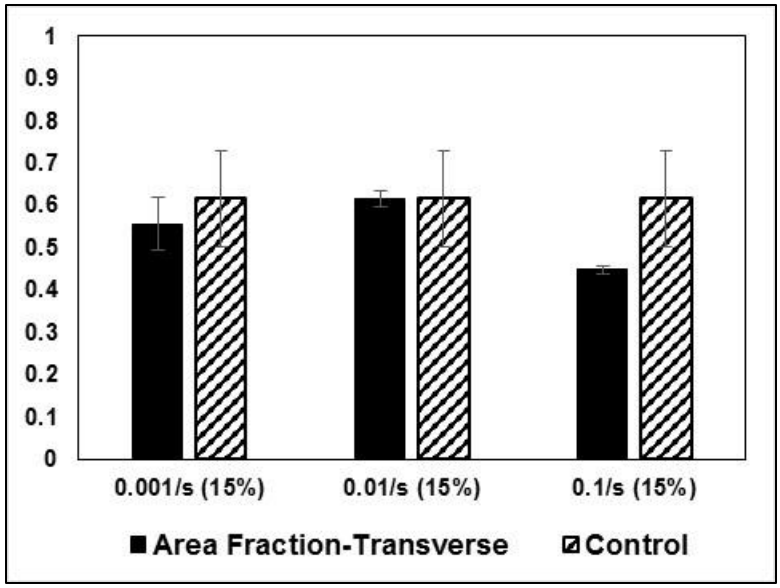

Figure 3.9 Area fraction of control and Transverse view at 15% strain

Similarly, the Figure 3.9 shows the Area fraction for all strain rates compared with the control at 15% strain in transverse direction. The area fraction of the cell cut in the transverse direction at 15% for all three strain rates 0.1/s,0.01/s and 0.001/s are 0.4469±0.0085, 0.61389±0.01866 and 0.55±0.0621 respectively. The area fraction for control is 0.615±0.113.

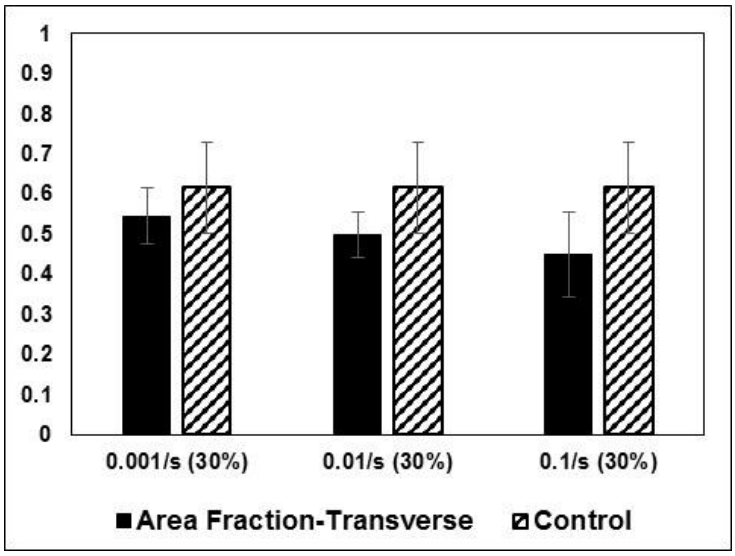

Figure 3.10 Area fraction of control and Transverse view at 30% strain

The area fraction of the cell cut in the transverse direction at 30% for all three strain rates 0.1/s,0.01/s and 0.001/s are 0.4469±0.0085, 0.61389±0.01866 and 0.55±0.0621 respectively.

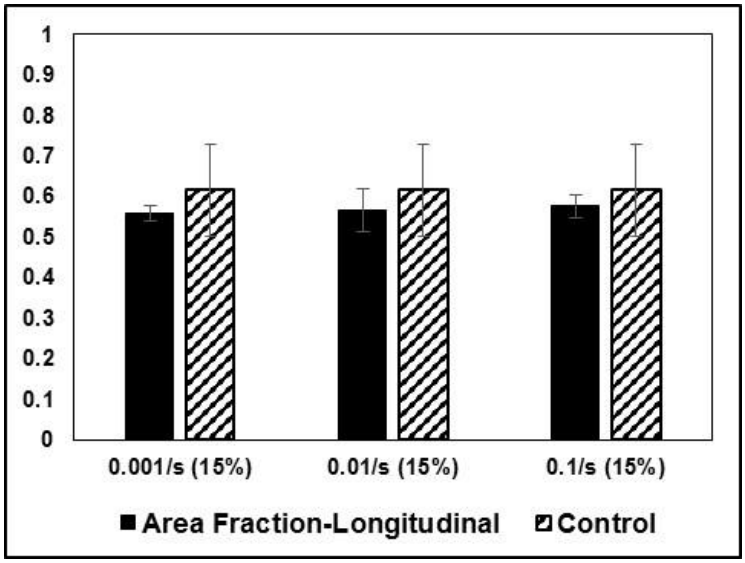

Figure 3.11 Area fraction of control and longitudinal view at 15% strain

The area fraction of the cell cut in the longitudinal direction at 15% for all three strain rates 0.1/s,0.01/s and 0.001/s are 0.57556±0.0277, 0.56475±0.05132 and 0.55638±0.018076 respectively. Area fraction for the control longitudinal is 0.615133±0.1129.

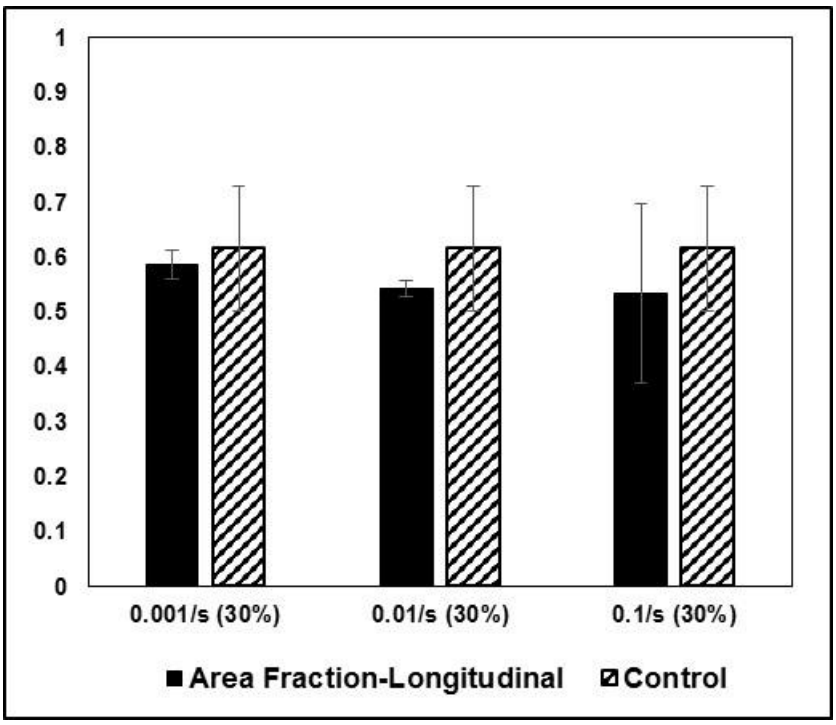

Figure 3.12 Area fraction of control and longitudinal view at 30% strain

The area fraction of the cell cut in the Longitudinal direction at 30% for all three strain rates 0.1/s,0.01/s and 0.001/s are 0.53378±0.16373, 0.5426±0.013966 and 0.58667±0.256 respectively.

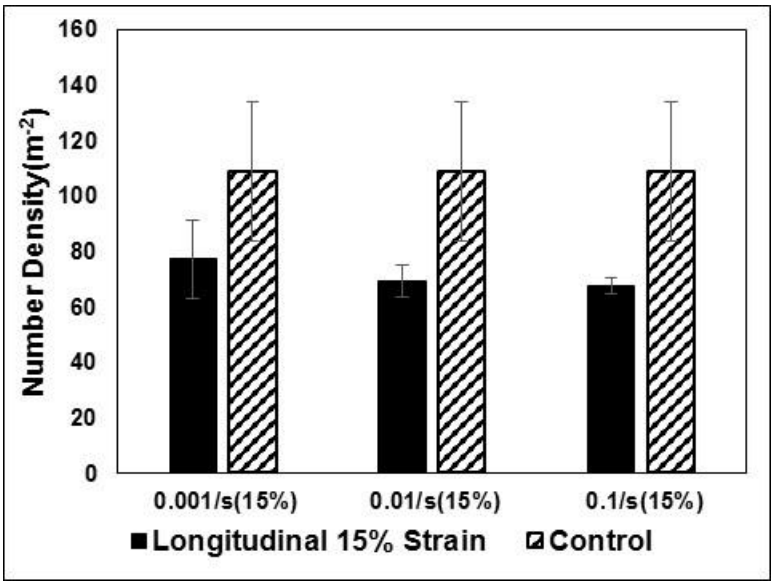

Figure 3.13 Number density of control and Longitudinal view at 15%

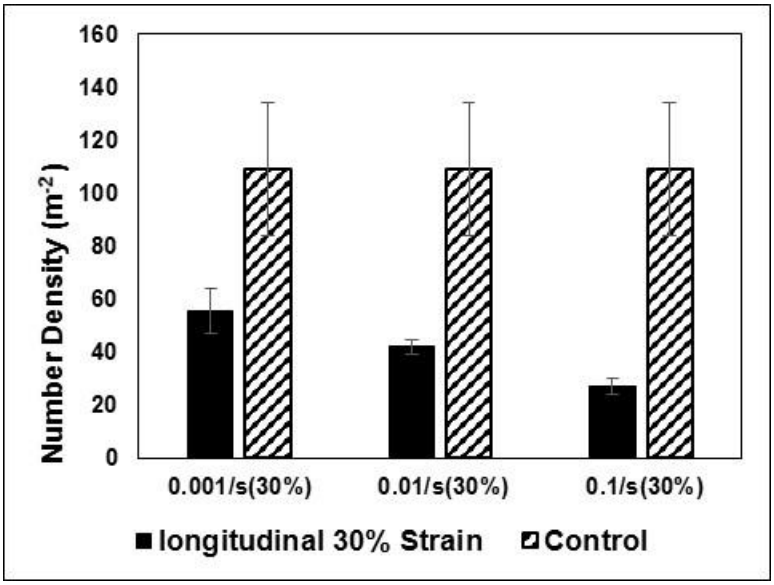

Figure 3.14 Number density of control and Longitudinal view at 30%

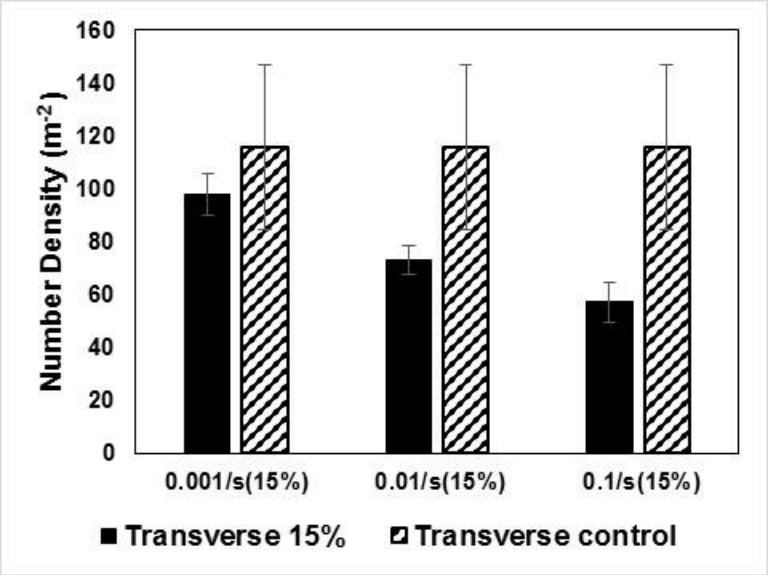

Figure 3.15 Number density of control and Transverse view at 15%

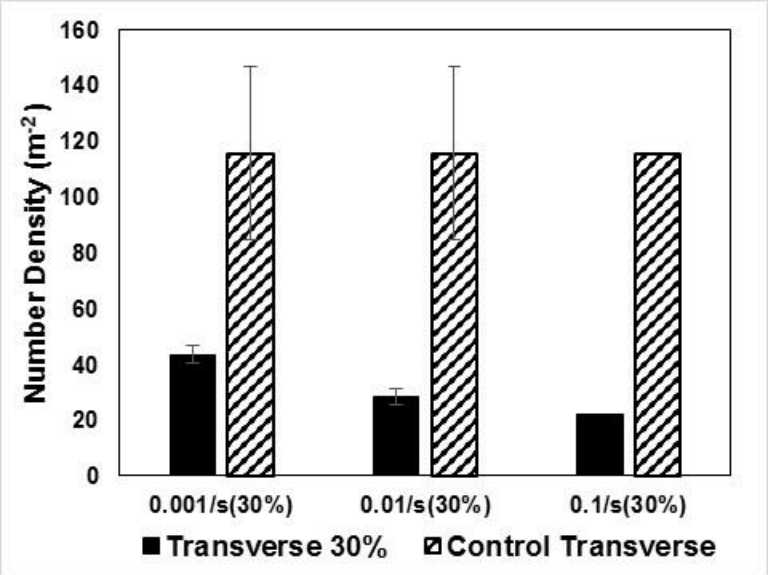

Figure 3.16 Number density of control and Transverse view at 30%

3.3 Histological Evaluation

Micrographs of Hematoxylin & Eosin stained cross section of fat with 0%(control), 15%(Longitudinal and transverse) and 30%(Longitudinal and transverse)for all three strain rates(0.1/s,0.01/s and 0.001/s) which are shown in Figure 3.17-Figure 3.28. Leica microscope show compression and change in the shape of the fat tissue. Figure 3.17-Figure 3.28 shows the disruption of the extracellular matrix as it is compressed while some are just flattened depending on the strain rates and strain percent.

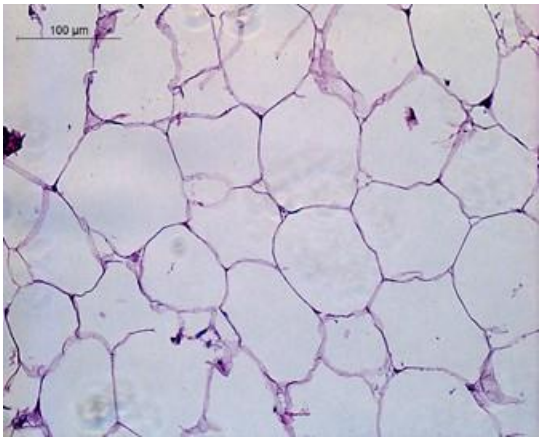

Figure 3.17 15% longitudinal view 0.01/s strain rates

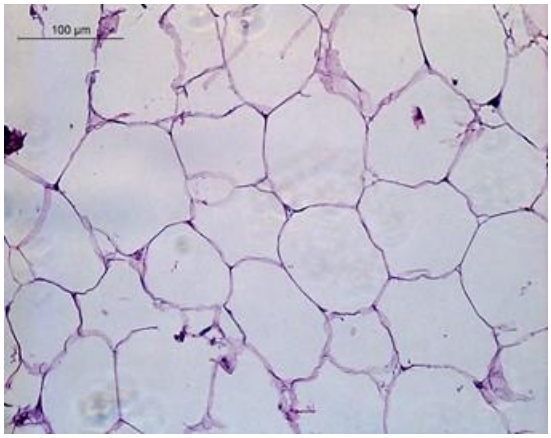

Figure 3.18 15% Transverse view at 0.01/s Strain rates

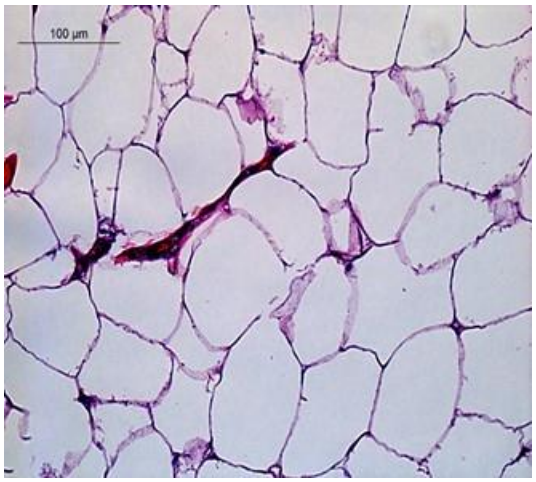

Figure 3.19 15% longitudinal view 0.1/s strain rates

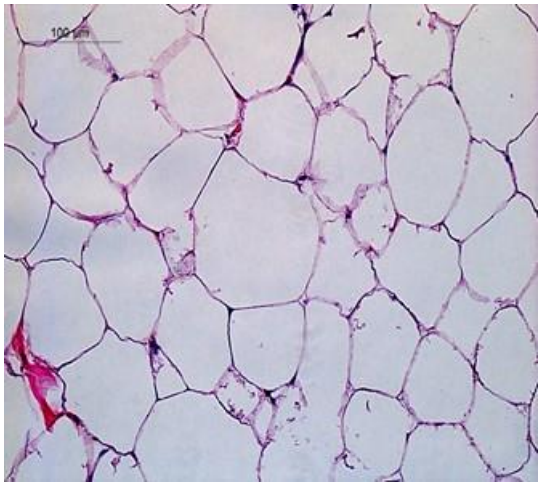

Figure 3.20 15% Transverse view at 0.1/s Strain rates

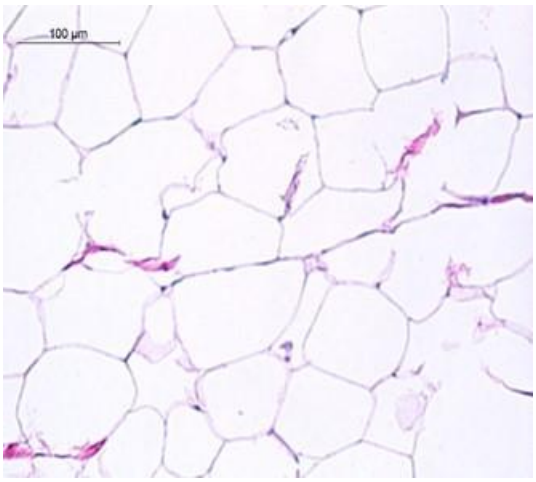

Figure 3.21 15% longitudinal view 0.001/s strain rates

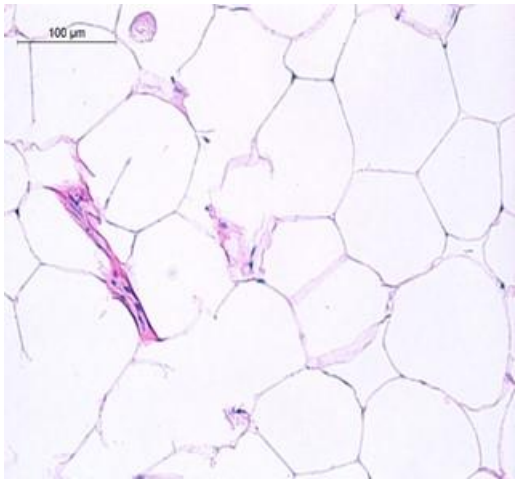

Figure 3.22 15% Transverse view at 0.001/s Strain rates

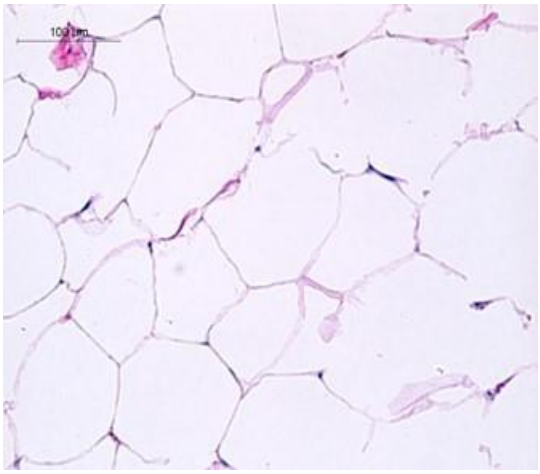

Figure 3.23 30% longitudinal view 0.01/s strain rates

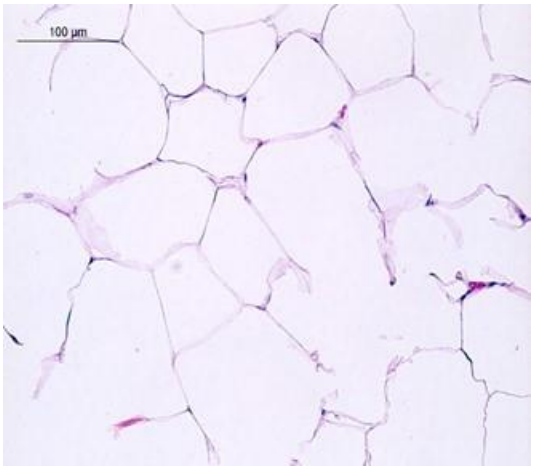

Figure 3.24 30% Transverse view at 0.01/s Strain rates

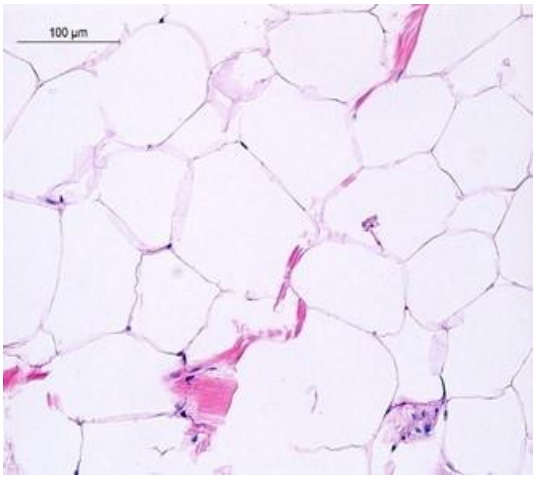

Figure 3.25 30% longitudinal view 0.001/s strain rates

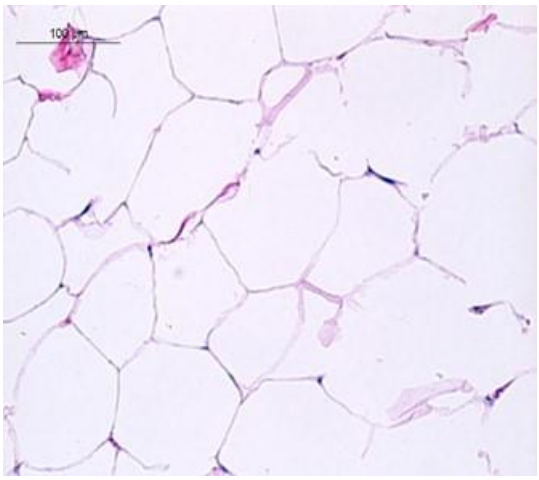

Figure 3.26 30% Transverse view at 0.001/s Strain rates

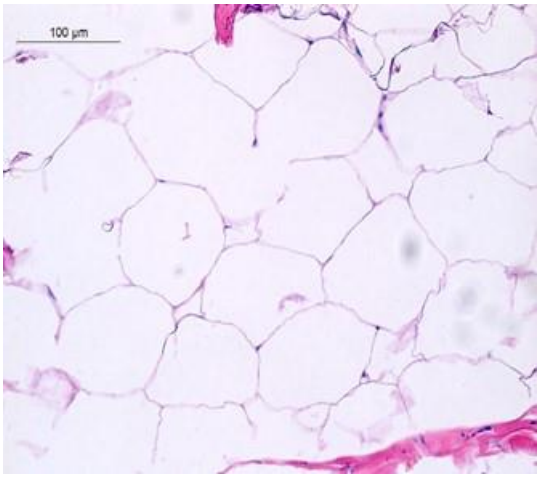

Figure 3.27 30% longitudinal view 0.1/s strain rates

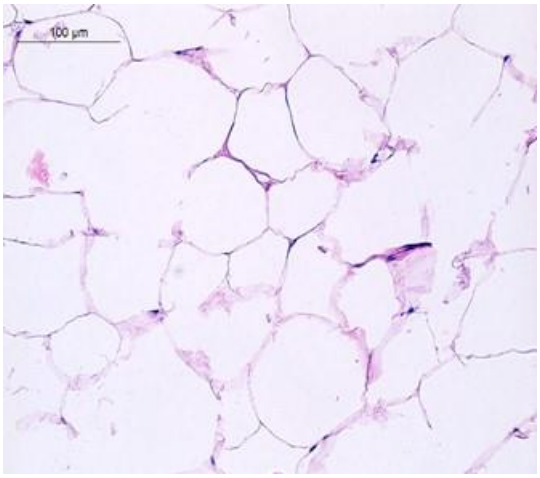

Figure 3.28 30% Transverse view at 0.1/s Strain rates

3.4 Hysteresis

Loading and unloading test were done on n=9 samples (n=3 for each strain rates) and up to 10 repetitive cycles. For each of the three strain rates of 0.1/s,0.001/s and 0.001/s fat tissue was compressed to 50% strain. Area of hysteresis loop was calculated using the MatLab software for each different cycle. From Table 2, the change in percentage from first loop and last loop is 75.56 at 0.1/s, 77.614 at 0.01/s and 91.423 at 0.001/s strain rates.

Table 3.2 Area of hysteresis loop for each separate cycle for all strain rates

Strain Rates	Area of 1st loop	Area of 2nd loop	Area of 3rd loop	Area of 8th loop	Area of 9th loop	Area of 10th loop	Change in % of 1st and 10th loop
0.1/s	12128	5379	4464	3242	3176	3142	75.56%
0.01/s	46952	19931	16318	11549	11071	10735	77.614%
0.001/s	53601	11758	8743	5169	4841	4587	91.423%

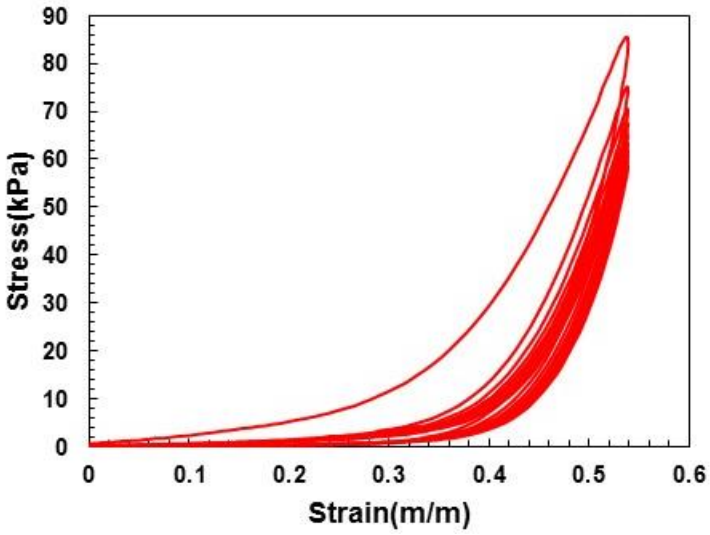

Figure 3.29 Hysteresis diagram of fat tissue at 0.1/s strain rate

Figure 3.29 shows the hysteresis loop for 0.1/s strain rates. The fat tissue was compressed repetitively keeping the strain constant for 10 different cycle. Similarly Figure 3.30 and Figure 3.31 shows the hysteresis loop of 0.01/s strain rate and 0.001/s strain rate respectively. The area of dissipation for 1st curve in 0.001/s strain rate is higher while at 0.1 is very smaller. When the sample is unloading in 0.1/s strain rate, the sample reaches to zero at around 35% strain and continued at zero strain until zero stress is obtained. Similarly, zero strain was reached during unloading at around 50% strain at 0.01/s strain rate. While at 0.001/s strain rate, during unloading, zero strain was obtained at 40% Strain.

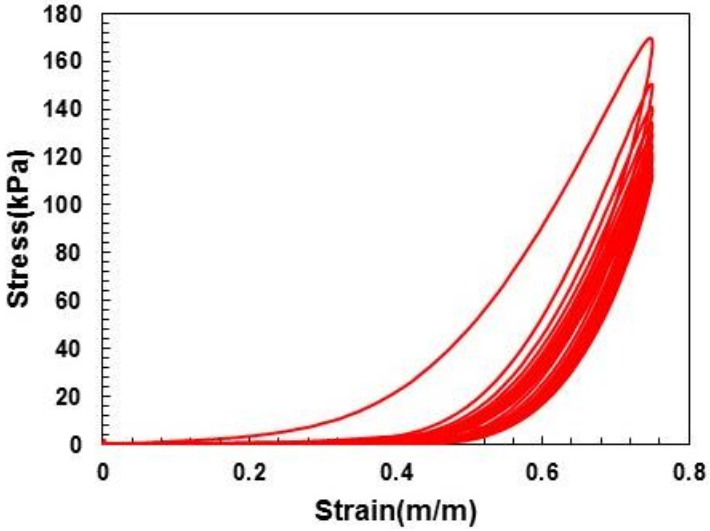

Figure 3.30 Hysteresis diagram of fat tissue at 0.01/s strain rate

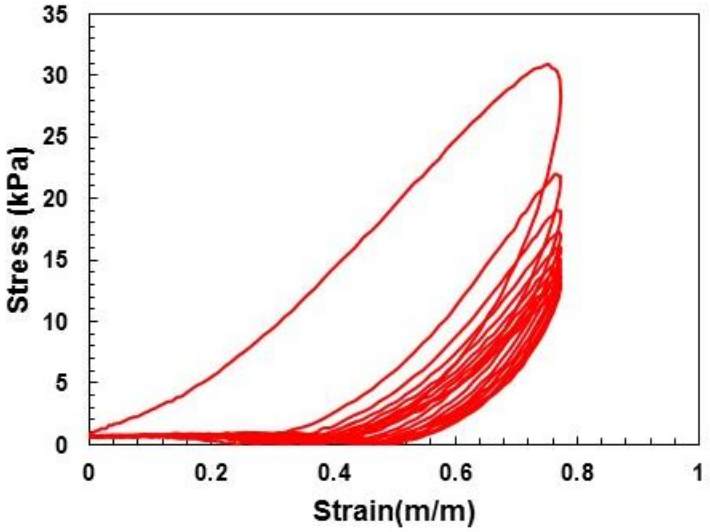

Figure 3.31 Hysteresis diagram of fat tissue at 0.001/s strain rate

CHAPTER IV

DISCUSSION

4.1 Viscoelastic Properties

Non-Linearity and viscoelasticity is the characteristic response of soft biological tissue. Fat tissue display a hysteresis loop formed by loading and unloading curve (Figure 3.29, Figure 3.30, and Figure 3.31).The curve for all three strain rates are slightly different for loading and unloading due to its stiffness. Cyclic loading and unloading were performed at all three different strain rate. The results from loading and unloading of fat tissue at 0.1/s, 0.001/s and 0.01/s strain rate showed that at lower strain, fat can dissipate more energy while at higher strain rate it can dissipate low energy. The area of dissipation is different in each cycle of loading and unloading. The area under the curve for all strain rates are also different, Plasticity can be seen in different strain values where zero stress was obtained in loading and unloading of the curve. (Sommer, Eder et al. 2013). As shown in Figure 3.29, Figure 3.30, Figure 3.31, the area under the curve for 0.1/s strain rate is lower than the area inside the loading and unloading curve for 0.01/s which is lower than 0.001/s strain rate. So, as the strain rate increases, fat tissue dissipate less energy.

Change in percentage from the 1st hysteresis loop to the last hysteresis loop(10th loop) is higher at low strain rates while it is lower at high strain rates as shown in Table 3.2. This might happen while fat tissue were compressed at lower strain rate, it dissipated

more energy resulting less rupture in fat cell on the first cycle. As the repeated loading and unloading occurs, even at the lower strain rate before it could regain its original position, more cell started to rupture resulting lower area of dissipation. So, the difference in the change of percentage at lower strain rate is higher. At high strain rates maximum number of fat cells are ruptured even in the first cycle resulting lower change in percentage.

4.2 Compression test

Stress-Strain relationship were observed and the data were obtained for all three different strain rates in longitudinal direction in the fat tissue. The biological tissue vary in response to strain depending on the nature and size. The non-linearity can be clearly seen after 20% as in Figure 3.1. The initial linear region shows that most of the fat or fluid has been expelled out. As the strain increases, more fluids are expelled from the fat tissue. The curve for 0.001/s strain rate is less stiff than the curve for 0.1/s strain rate. So, at low strain rate, fat tissue can dissipate more energy than the fat at higher strain rate with similar dimension. At same strain, lower strain rates can withstand higher stress while at higher strain rate, it can withheld comparatively low stress. As the fat tissue are compressed, the extra cellular matrix of fat cell ruptures decreasing the number of cell as shown in Table 3.1 .The number density is more at control while it is slightly less at 15% which is more less at 30%. Also cell density of longitudinal view when compressed in longitudinal direction is more than transverse view in all strain rates and in all strain. It has more difference at 30% strain rather than at 15% strain. When the cells are compressed longitudinally, the cells inside the extracellular matrix tries to move in the

transverse direction. So, at higher strain, in transverse view more cells are ruptured and elongated than in longitudinal view.

4.3 Microstructural Analysis

The stress strain response shows some effect in internal change in microstructure as a result of compression test. H&E staining was used to observe the changes in fat cell, in both transverse and longitudinal direction. Area fraction of longitudinal and transverse direction at three different strain rates(0.1/s,0.02/s,0.001/s) at 0%,15% and 30% strain values as shown from Figure 3.9-Figure 3.12 respectively.

In transverse direction at high strain rates area fraction is less than that at low strain rates compared to control but it depends on the size of the sample. Since all the sizes of sample were not same, some data may vary in that case. In both cases that is longitudinal and transverse direction, Area fraction from 0% to 30% strain decreases as strain rate increases. But some sample showed slightly different result due to vary in sample size and thickness.

As we can see the difference in the Figure 3.17-Figure 3.28, the H& E stained images shows that there are comparatively less number of cells as the strain increases. That is at 0% there are lots of number of cells while at 15% number of cells decreases. The number of cells is less at 30%. While at 0.001/s more number of cells compared to 0.01/s and 0.01/s as you can see in Figure 3.5-Figure 3.8. There is a difference in number of cells in transverse and longitudinal view. Longitudinal direction and transverse direction of control is same in number cells, number density and Area fraction while at different strain and different strain rate it is different.

CHAPTER V

CONCLUSION

This study has worked on quantifying the mechanical response of adipose tissue at various strain rates in compression. We have correlated the mechanics to the structural change occurring while under compression. The microstructural analysis such as number density and area fraction helps to design an engineering system like bioinspired material. Future work will consist of completing tensile test and compressing it in horizontal direction. Microstructural analysis will be needed in tensile test and hysteresis loop to verify the structure property relationship as well as to capture the percentage of elongation and percentage of cell rupture. Finding some mathematical model and relation using the experimental result. Also high rate stress strain response will be necessary for high rate impact validation. This test is a uniaxial testing so this test does not addresses any time dependent property of the tissue.

REFERENCES

Abraham, T. M., et al. (2015). "Association between visceral and subcutaneous adipose depots and incident cardiovascular disease risk factors." Circulation **132**(17): 1639-1647.

Aerts, P., et al. (1995). "The mechanical properties of the human heel pad: a paradox resolved." Journal of biomechanics **28**(11): 1299-1308.

Alkhouli, N., et al. (2013). "The mechanical properties of human adipose tissues and their relationships to the structure and composition of the extracellular matrix." American Journal of Physiology-Endocrinology and Metabolism **305**(12): E1427-E1435.

Cahill, G. F. and A. E. Renold (1965). Adipose tissue, Washington : American Physiological Society, 1965.

Comley, K. and N. Fleck (2012). "The compressive response of porcine adipose tissue from low to high strain rate." International Journal of Impact Engineering **46**: 1-10.

Comley, K. and N. A. Fleck (2010). "A micromechanical model for the Young's modulus of adipose tissue." International Journal of Solids and Structures **47**(21): 2982-2990.

Delingette, H. (1998). "Toward realistic soft-tissue modeling in medical simulation." Proceedings of the IEEE **86**(3): 512-523.

Geerligs, M., et al. (2008). "Linear viscoelastic behavior of subcutaneous adipose tissue." Biorheology **45**(6): 677-688.

Gefen, A. and E. Haberman (2007). "Viscoelastic properties of ovine adipose tissue covering the gluteus muscles." Journal of biomechanical engineering **129**(6): 924-930.

Iivarinen, J. T., et al. (2014). "Experimental and numerical analysis of soft tissue stiffness measurement using manual indentation device–significance of indentation geometry and soft tissue thickness." Skin Research and Technology **20**(3): 347-354.

Ker, R., et al. (1989). "Foot strike and the properties of the human heel pad." Proceedings of the Institution of Mechanical Engineers, Part H: Journal of Engineering in Medicine **203**(4): 191-196.

Kershaw, E. E. and J. S. Flier (2004). "Adipose tissue as an endocrine organ." The Journal of Clinical Endocrinology & Metabolism **89**(6): 2548-2556.

Miller-Young, J. E., et al. (2002). "Material properties of the human calcaneal fat pad in compression: experiment and theory." Journal of biomechanics **35**(12): 1523-1531.

Naemi, R., et al. (2015). "A mathematical method for quantifying in vivo mechanical behaviour of heel pad under dynamic load." Medical & biological engineering & computing: 1-10.

Patel, P. N., et al. (2005). "Rheological and recovery properties of poly (ethylene glycol) diacrylate hydrogels and human adipose tissue." Journal of biomedical materials research Part A **73**(3): 313-319.

Šifta, P. and V. Bittner (2010). Measurement of Reologic Properties of Soft Tissue (Muscle Tissue) by Device Called Myotonometer. 6th World Congress of Biomechanics (WCB 2010). August 1-6, 2010 Singapore, Springer.

Sommer, G., et al. (2013). "Multiaxial mechanical properties and constitutive modeling of human adipose tissue: a basis for preoperative simulations in plastic and reconstructive surgery." Acta biomaterialia **9**(11): 9036-9048.

Tan, E., et al. (2005). "Tensile testing of a single ultrafine polymeric fiber." Biomaterials **26**(13): 1453-1456.

Tracy, R. and P. Walia (2002). "A method to fix lipids for staining fat embolism in paraffin sections." Histopathology **41**(1): 75-79.

Wang, S. C., et al. (2003). Increased depth of subcutaneous fat is protective against abdominal injuries in motor vehicle collisions. Annu Proc Assoc Adv Automot Med.

Wertheimer, E. and B. Shapiro (1948). "THE PHYSIOLOGY OF ADIPOSE TISSUE." Physiological Reviews **28**(4): 451-464.

Williams, L. N., et al. (2008). "Variation of diameter distribution, number density, and area fraction of fibrils within five areas of the rabbit patellar tendon." Annals of Anatomy-Anatomischer Anzeiger **190**(5): 442-451.

Wu, J. Z., et al. (2007). "Simultaneous determination of the nonlinear-elastic properties of skin and subcutaneous tissue in unconfined compression tests." Skin Research and Technology **13**(1): 34-42.

APPENDIX A

CRYOFIXATION TECHNIQUE

Sample were taken out from internal muscle of porcine and cut in parallel to fiber (longitudinal) and perpendicular to the fiber (Transverse) direction. They were compressed in Biomomentum uniaxial MACH-1™ testing machine (Biomomentum Inc., Canada) with a 10 kg load cell and all tests were completed within five hours of post mortem to avoid rigor effects. Five cryofixation technique has been used for muscle of porcine. The technique used for cryofixation are dry ice, Isopentane, nitrogen, nitrogen with talcum powder and Glutaraldehyde. These cryofixed sample were stained with Hematoxylin and eosin staining. Images were obtained from using Leica Microscope. The obtained images were analyzed, from which the isopentane technique was found to be the best. Those images were further analyzed using the Image J software(NIH).

The number of pores, Area of pores, Area of muscle fiber and Area of matrix were calculated. The figures from A.1 to A.8 are the results obtained from the image J software. The results were analyzed for control, transverse and longitudinal direction. The strain used for study was 30% and 50%.

The results obtained does not satisfy to the previous studies result which showed isopentane is the best way for cryofixation. While looking at H and E staining images from microscope, they don't have more pores and formation of crystal. The slides used to study images were 3-4 years old which might be the reason for not satisfying the result that the isopentane is the best way to cryofix the tissue.

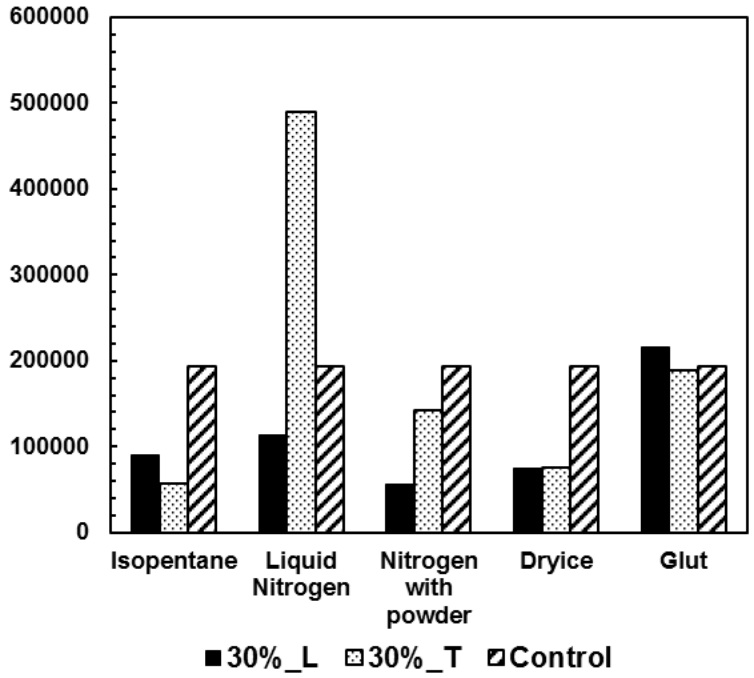

Figure A.1 Area of matrix at 30%for all five technique

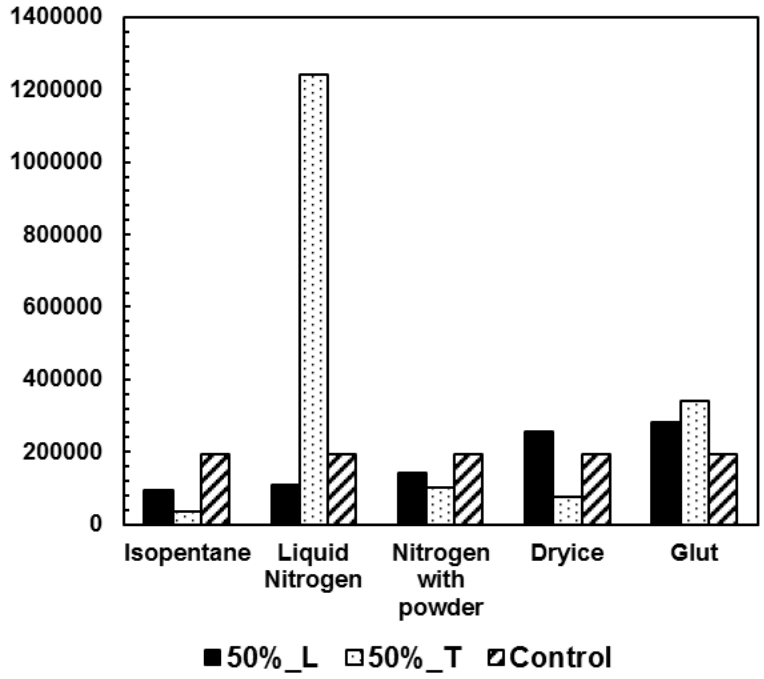

Figure A.2 Area of matrix at 50% for all five technique

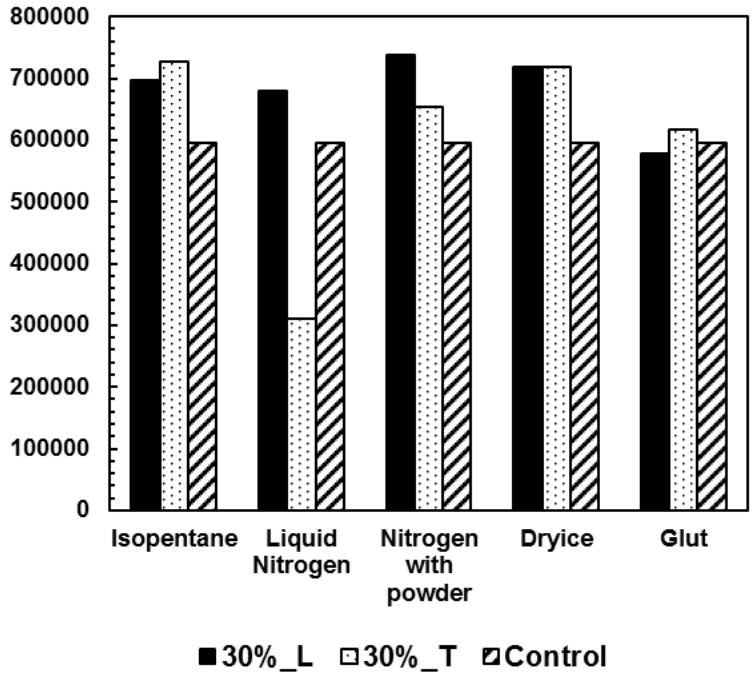

Figure A.3 Area of muscle fiber at 30% in longitudinal and transverse direction

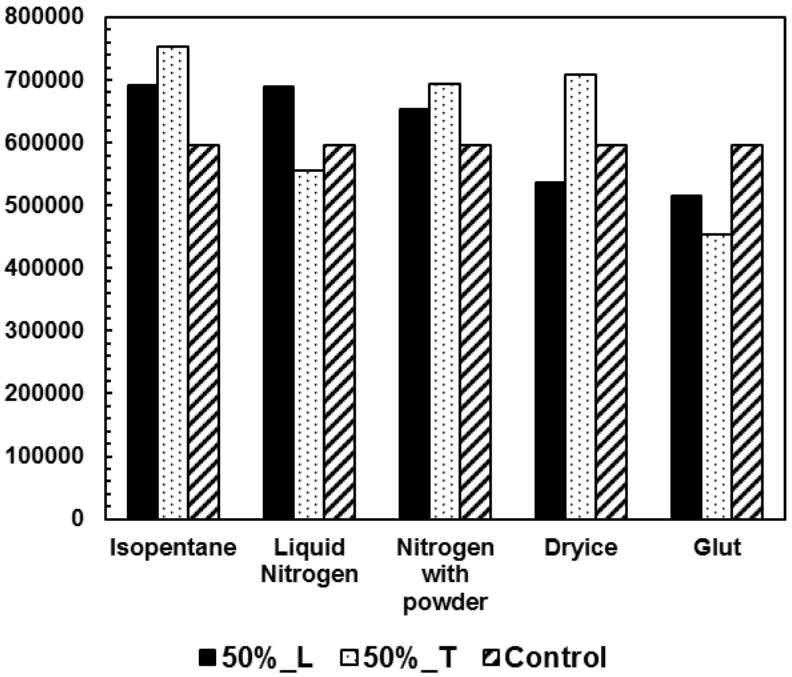

Figure A.4 Area of muscle fiber at 50% in longitudinal and transverse direction

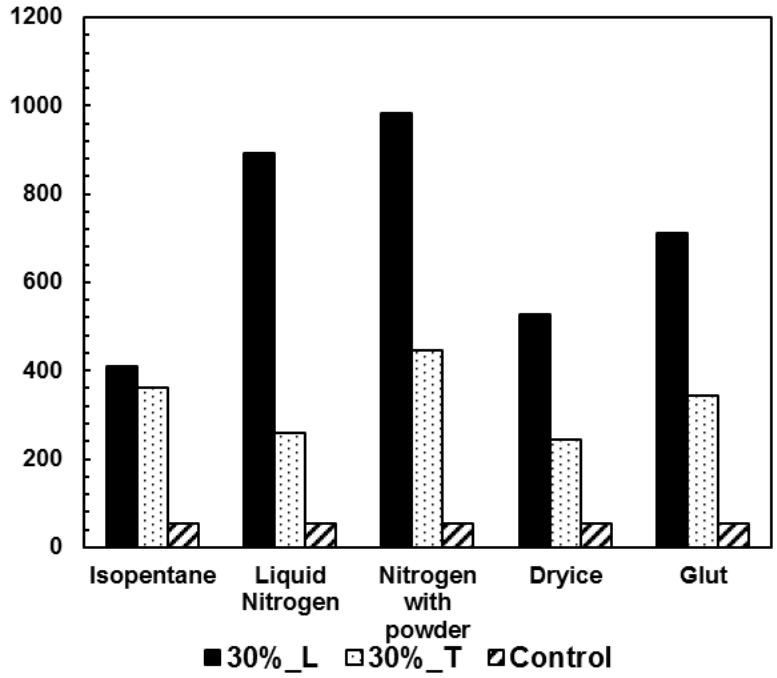

Figure A.5 Number of pores at 30% for all five technique in longitudinal and transverse direction

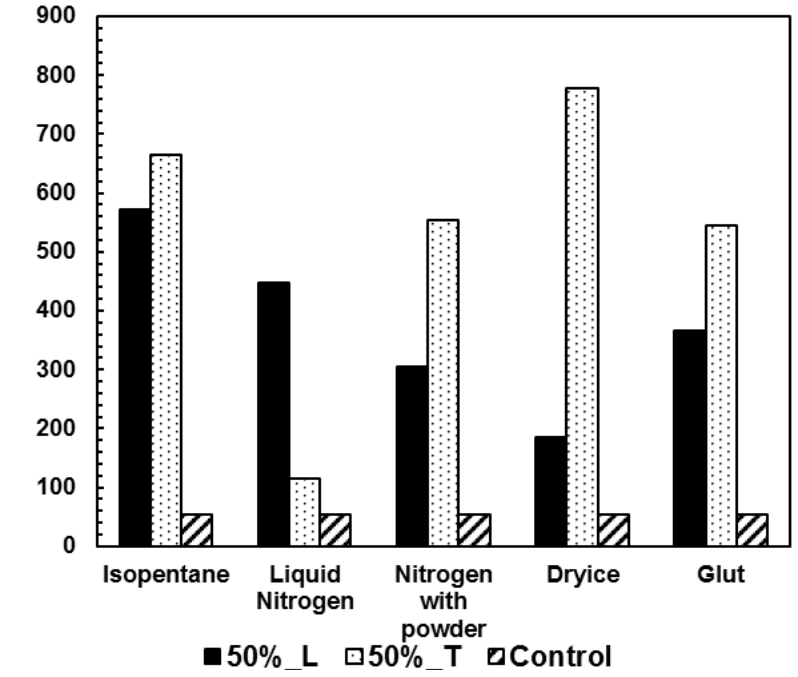

Figure A.6 Number of pores at 50% in longitudinal and transverse direction

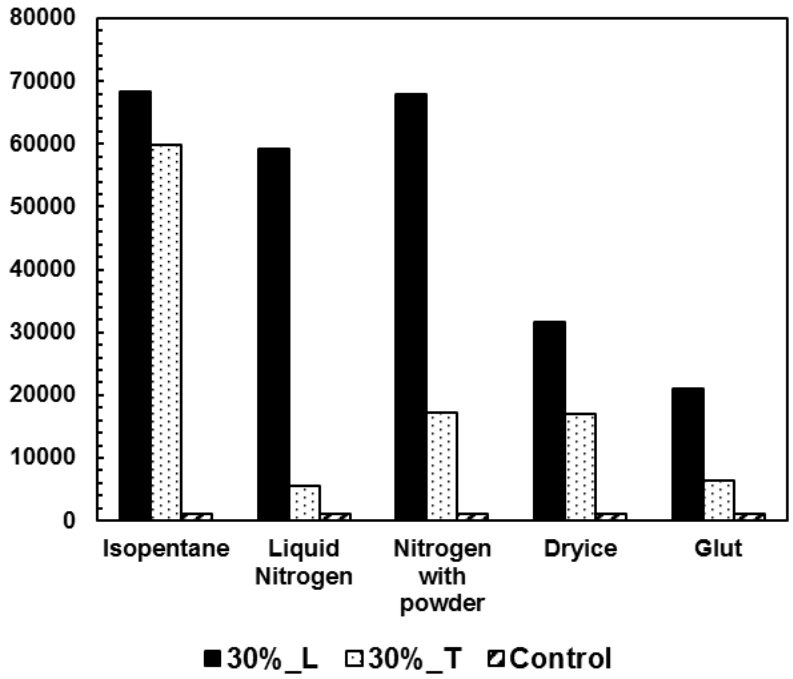

Figure A.7 Area of pores at 30% in longitudinal and transverse direction.

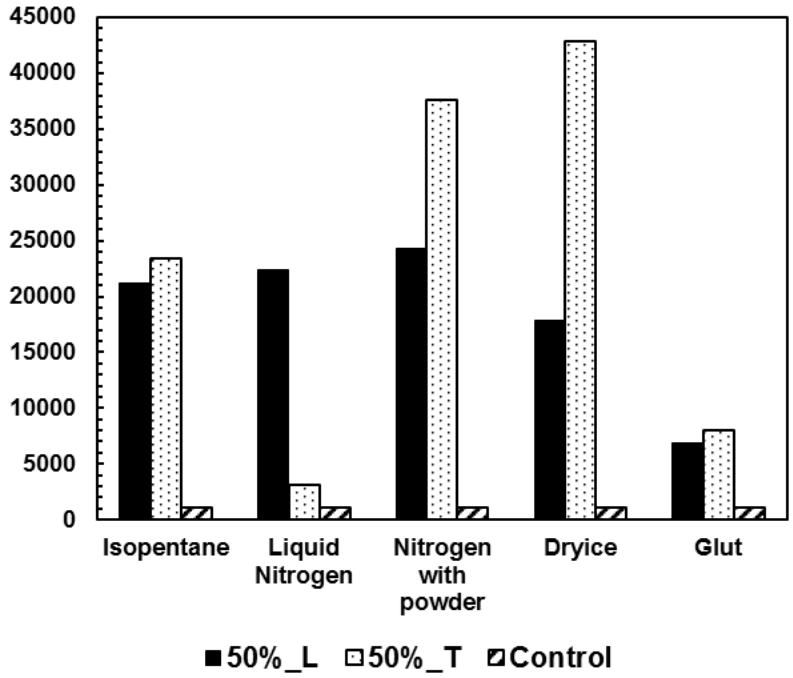

Figure A.8 Area of pores at 50% in longitudinal and transverse direction